Response prediction and parameter identification for base-isolated buildings with limited sensors

2015 NZSEE Conference

C. Zhou, J.G. Chase, G.W. Rodgers, A. Kuang & S. Gutschmidt

Department of Mechanical Engineering, University of Canterbury, Christchurch

C. Xu

School of Astronautics, Northwestern Polytechnical University, Xi'an, China

ABSTRACT: This research investigates the method of parameter identification for base-isolated buildings with a limited number of sensors. The base-isolated superstructure is considered as separated substructure from the isolation layer that shifts the natural frequency of the building away from the dominant frequency components of the ground motion, and is thus modelled as a shear type linear model. The structural response for the unrecorded floors are first predicted using a system of simultaneous linear equations with unknown parameters presented. Then a Gauss-Newton algorithm, which is based on solving a sequence of linearization least squares approximations to the nonlinear least square problems, is employed to identify the story stiffness and Rayleigh damping coefficients of the structure.

The performance and robustness of the proposed identification method is demonstrated using a simulated structure and different initial guesses, both with and without added noise. The numerical results show that the estimated story stiffness and damping coefficients converge to the exact value using different initial guesses without measurement noise, and are robust to noise with the average error within 16% even with 10% added noise. Finally, the estimated response for unrecorded floor are compared to the true response. The results indicate that the method is capable of predicting the structural response of the base-isolated building accurately using limited sensors.

1 INTRODUCTION

The isolation of structures from the ground motion is an effective way to protect the structure from damage in a strong earthquake. The basic concept of base isolation is to provide a low lateral stiffness between the structure and the foundation to lengthen the nature period of the building from its fixed-base value, moving the period away from the dominant period of the seismic ground motion. Thus, the transition of the earthquake motion and force to the superstructure of the isolated building can be significantly reduced.

Successful field performance of base isolated buildings was first recorded and validated in the University of South California Hospital building during the 1994 Northridge earthquake (Nagarajaiah and Sun 2000). Due to the lead rubber bearing isolation system, peak roof acceleration was reduced to 50% of the foundation acceleration, and the peak drift of the superstructure was less than 30% of the code specification. The measured response of two high damping rubber bearing isolated buildings in Miyagi and Chiba, Japan were investigated during the 2011 Tohoku earthquake (Miwada et al. 2012). The study confirmed acceleration reductions in both buildings, and the maximum accelerations at the floor above the isolated layer were 41%-83% of those in the basement. The strong motion seismic records of Fukushima Dai-Ichi Nuclear Power Plant were also reported in the Great East Japan earthquake in 2011 (Hijikata et al. 2011). The base isolated structure performed well in horizontal motion with the response reduced by 30% from the basement pit.

A number of researchers have investigated the system identification methods for base isolated buildings using different system models. Stewart et al. (1999) identified the structural modal parameters of four base isolated buildings using an equivalent time-varying linear model, based on the assumption of the superstructure as a SODF system and the isolation system with time-varying effective stiffness, to characterize the isolation performance during the earthquake. Furukawa et al. (2005) proposed a least squares output-error minimization method to identify a base-isolated building affected by the 1995 Hyogoken-Nambu earthquake in Japan. The superstructure was modelled as a rigid body and the isolation system was identified based on three different models: a linear equivalent model, a bilinear model and a trilinear model. Results show that the model parameters can be reasonably estimated and the trilinear model best fit the recorded response time histories.

Huang et al. (2009) developed an iterative trial-and-error optimization procedure, based on a simplified bilinear model for the base isolation system and a multi-story linear model for the superstructure. They identified the structural parameters of a base isolated building using a Masing criterion to transform a multi-valued hysteretic restoring force function into a single-valued function so that ordinary optimization method can be applied. Xu et al. (2014) recently proposed a two-step regression analysis procedure to identify the physical parameters of a base isolated structure. A bilinear model was chosen for modelling the base isolator and the superstructure was assumed as a single degree of freedom system. The hysteresis loop was divided into different half cycles according to the zero velocity points and multiple linear regression was applied to those half cycles to yield equivalent linear system stiffness and damping.

For all these system identification methods, a key element is the choice of proper models for the base isolation system and superstructure. The choice is primarily based on the actual or expected response of the building and isolators, and is critical for accurate identification. Since the isolated building should be quite rigid in comparison to the isolation system, a superstructure is frequently assumed to be a lumped mass that reduces the computational efforts significantly (Kulkarni and Jangid 2002). Otherwise, a multi-story linear model is considered for the superstructure (Kulkarni and Jangid 2003). For the base isolation system, a nonlinear hysteretic model (Park et al. 1986) is widely used to characterize the nonlinear force-deformation behaviour of the lead rubber bearings experiencing the inelastic seismic response expected by design (Gavin and Wilkinson 2010, Matsagar and Jangid 2008). However, the properties of lead rubber bearing can be modelled using a spring equivalent linear horizontal stiffness in the case that the ground motion is not very large or the base isolation system has no yielding under the ground shaking (Chen et al. 2007). Hence, the isolation layer response may vary from the expected performance or have a range of behaviours, and thus have a significant, negative impact on the identified model's accuracy.

Christchurch Women's Hospital (CWH) building is the only base isolated building in the South Island of New Zealand. The performance of the instrumented CWH building was investigated using the recorded accelerations at the foundation, first and top level during two major earthquakes in 2011 (Kuang et al. 2014). The results indicate that the superstructure of the building does not approximate as a rigid body as might be expected. The base isolation system was still within the stiffer linear range and did not lead to the period separation of the ground shaking and the building during these events. Thus, a four degree of freedom linear shear model is used for the parameter identification of the CWH base isolated building with the accelerations recorded for the first and fourth degrees of freedom, as well as the ground motion inputs in the basement.

In this study, an identification method is proposed to identify the equivalent stiffness and Rayleigh damping for the four degree of freedoms linear system. The response for the unrecorded degree of freedom were estimated based on a simultaneous linear equations. A modified Gauss-Newton method was then employed to identify the equivalent stiffness and Rayleigh damping of the system. The performance of the proposed method is demonstrated and validated using a simulated structure. Robustness is investigated using different initial guesses and by added 10% RMS noise.

2 IDENTIFICATION METHOD

The equation of motion for the base-isolated building subject to seismic excitation is defined:

$$M\ddot{X} + C\dot{X} + KX = -MI\ddot{x}_g \tag{1}$$

where $X=[x_1\ x_2\ x_3\ x_4]^T$; the mass matrix $M=\text{diag}(m_1\ m_2\ m_3\ m_4)$; and the stiffness matrix K and Rayleigh damping matrix C are defined:

$$K = \begin{bmatrix} K_1+K_2 & -K_2 & 0 & 0 \\ -K_2 & K_2+K_3 & K_3 & 0 \\ 0 & -K_3 & K_3+K_4 & -K_4 \\ 0 & 0 & -K_4 & K_4 \end{bmatrix} \tag{2}$$

$$C = a_0 M + a_1 K_T = \begin{bmatrix} C_{11} & -C_{12} & 0 & 0 \\ -C_{21} & C_{22} & -C_{23} & 0 \\ 0 & -C_{32} & C_{33} & -C_{34} \\ 0 & 0 & -C_{43} & C_{44} \end{bmatrix} \tag{3}$$

Therefore, the equation of motion for the first and fourth DOFs at $t=t_i$ can be described using Equations (1)-(3):

$$f_{1i} = m_1(\ddot{x}_1 + \ddot{x}_g) + C_{11}\dot{x}_1 - C_{12}\dot{x}_2 + (K_1+K_2)x_1 - K_2 x_2 = 0 \tag{4}$$

$$f_{4i} = m_4(\ddot{x}_4 + \ddot{x}_g) - C_{43}\dot{x}_3 + C_{44}\dot{x}_4 - K_4 x_3 + K_4 x_4 = 0 \tag{5}$$

where and $\ddot{x}_1$, $\ddot{x}_4$ and $\ddot{x}_g$ are measured; the velocities $\dot{x}_1$, $\dot{x}_4$ and displacements x_1 and x_4 can be obtained by direct integration after band pass filtering (Boroschek et al. 2003, Chaudhary et al. 2000, Sridhar et al. 2014, Yang et al. 2003). Equations (4) and (5) can then be rewritten in terms of unknowns x_2 and x_3:

$$\dot{x}_2 + P_1(K_2, C_{12})x_2 = Q_1(K_1, K_2, C_{11}, C_{12}, t) \tag{6}$$

$$\dot{x}_3 + P_2(K_4, C_{43})x_3 = Q_2(K_4, C_{43}, C_{44}, t) \tag{7}$$

where:

$$P_1(K_2, C_{12}) = \frac{K_2}{C_{12}};\ \ Q_1(K_1, K_2, C_{11}, C_{12}, t) = \frac{m_1\ddot{x}_1 + C_{11}\dot{x}_1 + (K_1+K_2)x_1 + m_1\ddot{x}_g}{C_{12}} \tag{8}$$

$$P_2(K_2, C_{12}) = \frac{K_4}{C_{43}};\ \ Q_2(K_4, C_{43}, C_{44}, t) = \frac{m_4\ddot{x}_4 + C_{44}\dot{x}_4 + K_4 x_4 + m_4\ddot{x}_g}{C_{43}} \tag{9}$$

The general solutions for Equations (6) and (7) are:

$$x_2(t) = e^{-\int P_1(K_2, C_{12})dt}\left(A_i + \int Q_1(K_1, K_2, C_{11}, C_{12}, t)e^{\int P_1(K_2, C_{12})dt}dt\right) \tag{10}$$

$$x_3(t) = e^{-\int P_2(K_4, C_{43})dt}\left(B_i + \int Q_2(K_4, C_{43}, C_{44}, t)e^{\int P_2(K_4, C_{43})dt}dt\right) \tag{11}$$

For each time step $h=t_i-t_{i-1}$, the free terms Q_1 and Q_2 can be written as a moving average:

$$Q_{1i} = \frac{Q_1(K_1, K_2, C_{11}, C_{12}, t_{i-1}) + Q_1(K_1, K_2, C_{11}, C_{12}, t_i)}{2} \qquad t_{i-1} \le t \le t_i \tag{12}$$

$$Q_{2i} = \frac{Q_2(K_4, C_{43}, C_{44}, t_{i-1}) + Q_2(K_4, C_{43}, C_{44}, t_i)}{2} \qquad t_{i-1} \le t \le t_i \tag{13}$$

Hence, Equations (10) and (11) can be rewritten:

$$x_2(t) = e^{-(t-t_{i-1})/a_1}(A_i + a_1 Q_{1i} e^{(t-t_{i-1})/a_1}) \tag{14}$$

$$x_3(t) = e^{-(t-t_{i-1})/a_1}(B_i + a_1 Q_{2i} e^{(t-t_{i-1})/a_1}) \tag{15}$$

where A_i and B_i are constants determined by initial condition at $t=t_{i-1}$. If $x_2(t_{i-1})$ and $x_3(t_{i-1})$ are known from the prior time-step $t=t_{i-1}$, then the constants A_i and B_i can be determined using Equations (14) and (15):

$$A_i = x_2(t_{i-1}) - a_1 Q_{1i} \tag{16}$$

$$B_i = x_3(t_{i-1}) - a_1 Q_{2i} \tag{17}$$

Then from Equations (14)-(17), the complete estimates for $x_2(t_i)$ and $x_3(t_i)$ with sampling time interval $h=t_i-t_{i-1}$ are obtained iteratively given $x_2(0)$ and $x_3(0)$ to start:

$$x_2(t_i) = x_2(t_{i-1}) e^{-h/a_1} + a_1(1 - e^{-h/a_1}) Q_{1i} \tag{18}$$

$$x_3(t_i) = x_3(t_{i-1}) e^{-h/a_1} + a_1(1 - e^{-h/a_1}) Q_{2i} \tag{19}$$

Thus, the identification error function can be defined:

$$\varepsilon(\hat{\boldsymbol{\theta}}) = \sum_{i=1}^{n} f_{1i}(\hat{\boldsymbol{\theta}}) + \sum_{i=1}^{n} f_{2i}(\hat{\boldsymbol{\theta}}) + \sum_{i=1}^{n} f_{3i}(\hat{\boldsymbol{\theta}}) + \sum_{i=1}^{n} f_{4i}(\hat{\boldsymbol{\theta}}) \tag{20}$$

where n is the number of time step; $\boldsymbol{\theta}$= [K_1, K_2, K_3, K_4, a_0, a_1] is the parameter vector and identified by minimizing the error function using a Gauss-Newton formula:

$$\hat{\boldsymbol{\theta}}^{(s+1)} = \hat{\boldsymbol{\theta}}^{(s)} - \alpha(\mathbf{J}^{\mathbf{T}}\mathbf{J})^{-1}\mathbf{J}^{\mathbf{T}}\mathbf{R}^{(s)} \tag{21}$$

where s is the iteration time step, α is the step length and $\mathbf{J}$ is the Jacobian matrix of $f_i(\hat{\boldsymbol{\theta}}^{(s)})$:

$$\mathbf{J} = \begin{bmatrix} \mathbf{J}_1 & \cdots & \mathbf{J}_i & \cdots & \mathbf{J}_n \end{bmatrix}^{\mathbf{T}} \tag{22}$$

$$\mathbf{J}_i = \begin{bmatrix} \frac{\partial f_{1i}(\hat{\boldsymbol{\theta}}^{(s)})}{\partial K_1} & \frac{\partial f_{1i}(\hat{\boldsymbol{\theta}}^{(s)})}{\partial K_2} & \frac{\partial f_{1i}(\hat{\boldsymbol{\theta}}^{(s)})}{\partial K_3} & \frac{\partial f_{1i}(\hat{\boldsymbol{\theta}}^{(s)})}{\partial K_4} & \frac{\partial f_{1i}(\hat{\boldsymbol{\theta}}^{(s)})}{\partial a_0} & \frac{\partial f_{1i}(\hat{\boldsymbol{\theta}}^{(s)})}{\partial a_1} \\ \frac{\partial f_{2i}(\hat{\boldsymbol{\theta}}^{(s)})}{\partial K_1} & \frac{\partial f_{2i}(\hat{\boldsymbol{\theta}}^{(s)})}{\partial K_2} & \frac{\partial f_{2i}(\hat{\boldsymbol{\theta}}^{(s)})}{\partial K_3} & \frac{\partial f_{2i}(\hat{\boldsymbol{\theta}}^{(s)})}{\partial K_4} & \frac{\partial f_{2i}(\hat{\boldsymbol{\theta}}^{(s)})}{\partial a_0} & \frac{\partial f_{2i}(\hat{\boldsymbol{\theta}}^{(s)})}{\partial a_1} \\ \frac{\partial f_{3i}(\hat{\boldsymbol{\theta}}^{(s)})}{\partial K_1} & \frac{\partial f_{3i}(\hat{\boldsymbol{\theta}}^{(s)})}{\partial K_2} & \frac{\partial f_{3i}(\hat{\boldsymbol{\theta}}^{(s)})}{\partial K_3} & \frac{\partial f_{3i}(\hat{\boldsymbol{\theta}}^{(s)})}{\partial K_4} & \frac{\partial f_{3i}(\hat{\boldsymbol{\theta}}^{(s)})}{\partial a_0} & \frac{\partial f_{3i}(\hat{\boldsymbol{\theta}}^{(s)})}{\partial a_1} \\ \frac{\partial f_{4i}(\hat{\boldsymbol{\theta}}^{(s)})}{\partial K_1} & \frac{\partial f_{4i}(\hat{\boldsymbol{\theta}}^{(s)})}{\partial K_2} & \frac{\partial f_{4i}(\hat{\boldsymbol{\theta}}^{(s)})}{\partial K_3} & \frac{\partial f_{4i}(\hat{\boldsymbol{\theta}}^{(s)})}{\partial K_4} & \frac{\partial f_{4i}(\hat{\boldsymbol{\theta}}^{(s)})}{\partial a_0} & \frac{\partial f_{4i}(\hat{\boldsymbol{\theta}}^{(s)})}{\partial a_1} \end{bmatrix} \tag{23}$$

where $\mathbf{R}^{(s)}$ is the error matrix at iteration s:

$$\mathbf{R}^{(s)} = \begin{bmatrix} f_{11}(\hat{\boldsymbol{\theta}}^{(s)}) \cdots & f_{41}(\hat{\boldsymbol{\theta}}^{(s)}) & \cdots & f_{1i}(\hat{\boldsymbol{\theta}}^{(s)}) \cdots & f_{4i}(\hat{\boldsymbol{\theta}}^{(s)}) & \cdots & f_{1n}(\hat{\boldsymbol{\theta}}^{(s)}) \cdots & f_{4n}(\hat{\boldsymbol{\theta}}^{(s)}) \end{bmatrix}^{\mathbf{T}} \tag{24}$$

3 SIMULATION AND VALIDATION CASE STUDY

A numerical study is carried out to validate the performance of the proposed procedure in a controlled example where everything is known. The example structure is a four degree of freedom system with a set of parameters: m_1=3892e+3kg, m_2=12974e+3kg, m_3=2595e+3kg, m_4=3892e+3kg, K_1=728kN/mm, K_2=1120kN/mm, K_3=280kN/mm, K_4=300kN/mm. The Rayleigh damping coefficients are a_0=0.261 and a_1=0.0087, yielding damping ratio of 5% for the first and second modes. The simulated structure was subjected to the El Centro earthquake, 1940. The system response was simulated using a Runge Kutta integration method with a time step of Δt=0.005s.

The calculated response data was utilized without added noise first, for proof of concept of identification procedure. Figure 1 shows the estimates and convergence of the proposed parameters with different initial guesses for $K_{1\text{-}4}$ and $a_{0\text{-}1}$. It can be seen that the final values of the estimated parameters converge to the exact values with different initial guesses. Thus, the identification method can yield accurate estimates of equivalent stiffness and damping coefficients of the system with clean measurements.

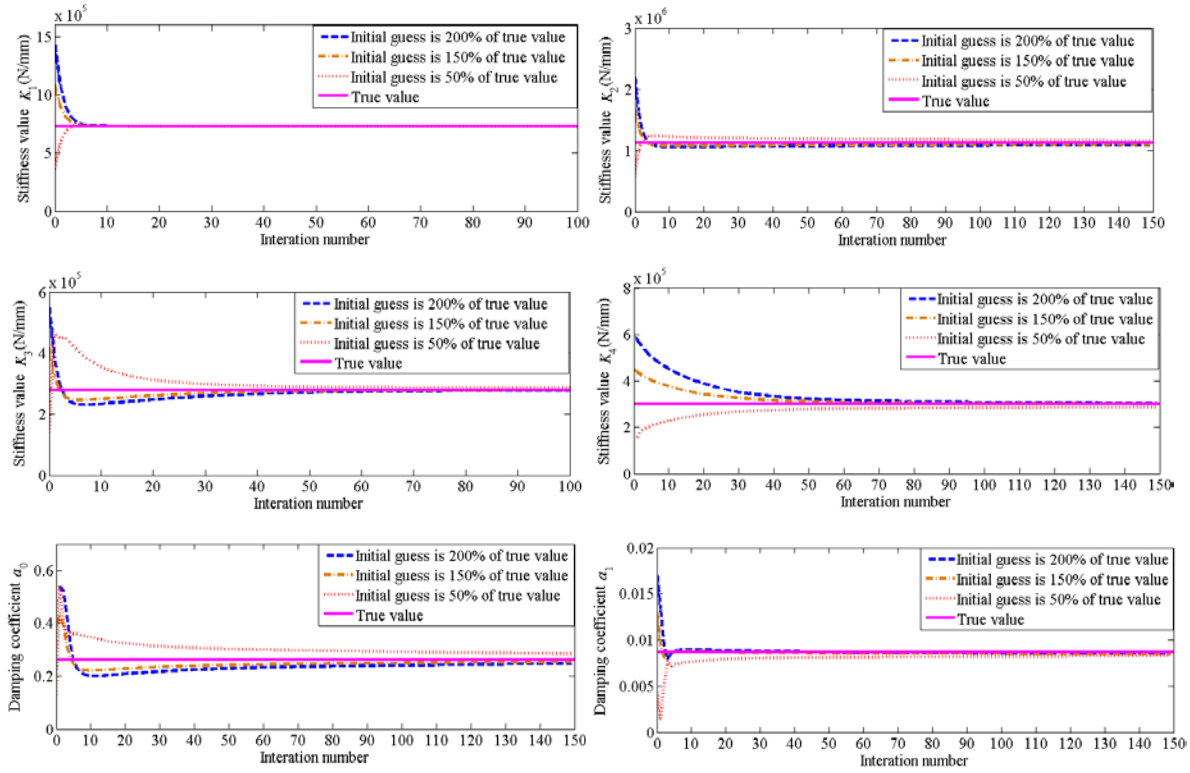

Figure 1. Parameter estimation performance with different initial guess values.

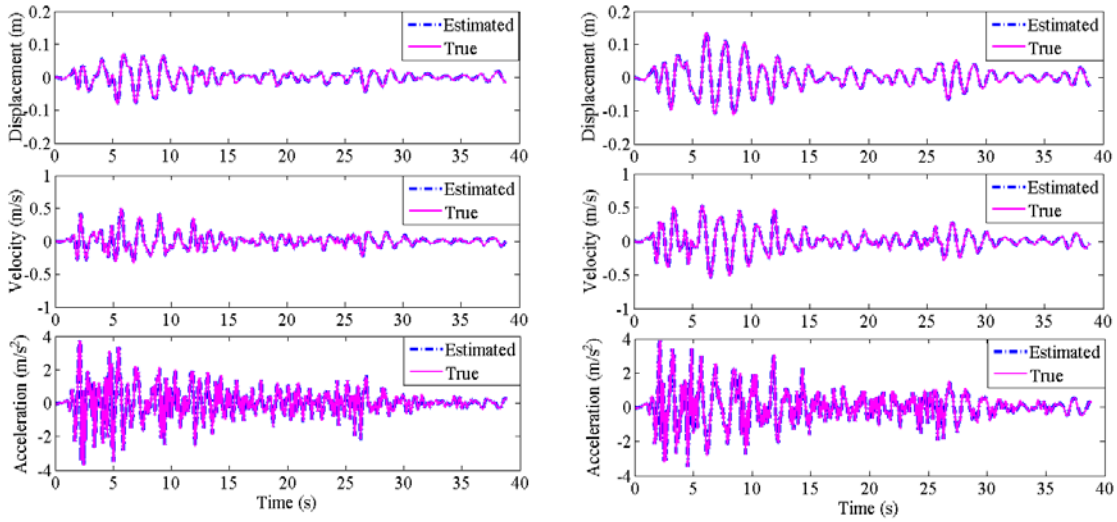

(a) **(b)**

Figure 2. Comparison of the estimated and true response for the unmeasured DOFs using initial guess 200% of exact parameter values: (a) 2nd DOF; (b) 3rd DOF.

Figure 2 compares the estimated response and true simulated response for x_2 and x_3 using an initial guess 200% of the exact structural parameter values. The estimated response matched well with the simulated response, which indicate the method can yield good estimates of the unrecorded response for x_2 and x_3 with clean (noise free) acceleration measurements of the first and fourth DOF.

To assess the robustness to noise, a 10% RMS noise was added to the measured ground and structural accelerations. The mean values of the estimated parameters for 100 Monte-Carlo runs with random added noise and different initial guesses, are shown in Table 1.

Table 1. Mean estimated results with 10% RMS noise for different initial guesses.

Parameters	K_1 (kN/mm)	K_2 (kN/mm)	K_3 (kN/mm)	K_4 (kN/mm)	a_0	a_1
Initial guess: 200% of true value	1456	2240	560	600	0.522	0.0174
Estimated value	738	1053	231	395	0.336	0.0093
True value	728	1120	280	300	0.261	0.0087
Monte-Carlo mean absolute error	1.4%	6.0%	17.5%	31.7%	28.7%	6.9%
Average error of parameters			16.6%			
Initial guess: 150% of true value	1092	1680	420	450	0.392	0.0131
Estimated value	734	1074	241	340	0.296	0.0091
True value	728	1120	280	300	0.261	0.0087
Monte-Carlo mean absolute error	0.8%	4.1%	13.9%	13.3%	13.4%	4.7%
Average error of parameters			8.7%			
Initial guess: 50% of true value	364	560	140	150	0.131	0.0044
Estimated value	670	1132	301	242	0.212	0.0093
True value	728	1120	280	300	0.261	0.0087
Monte-Carlo mean absolute error	8.0%	1.1%	7.5%	19.3%	18.8%	6.9%
Average error of parameters			11.5%			

The average error of the estimated parameters is 16.6% with the largest Monte-Carlo mean error 31.7% using an initial guess of 200% of exact parameter values. However, the average error of the parameters estimates decreases to 8.7% with the largest Monte-Carlo mean error 13.9% using initial guess of 150% of exact values and 11.5% with the largest Monte-Carlo mean error 19.3% using an initial guess of 50%. Thus, the initial guess affects identification accuracy with measurement noise. However, the estimated response using the estimated parameters shows good agreement with the true response for the unrecorded DOFs, even with 10% added noise using an initial guess of 200% of exact parameters values, as shown in Figure 3.

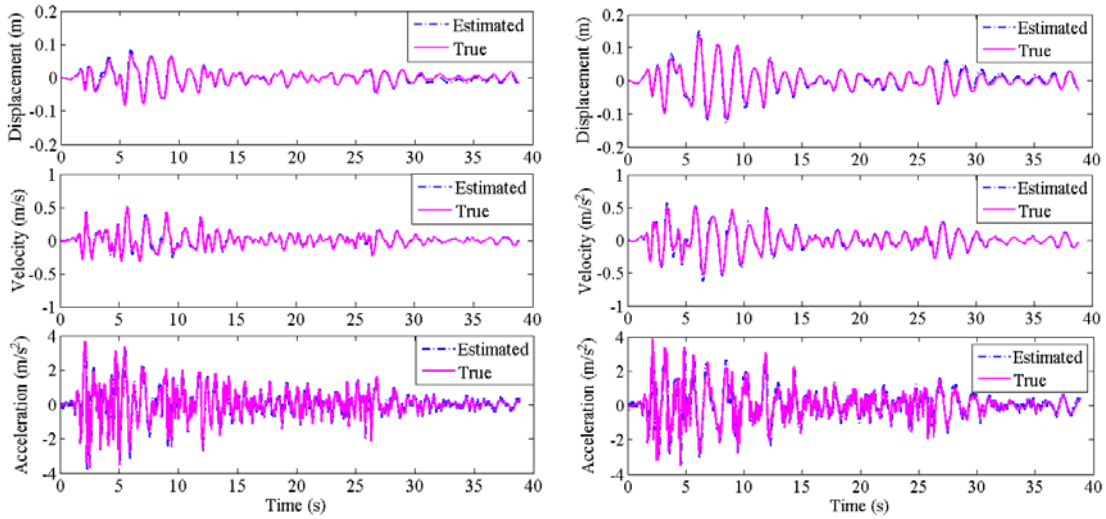

Figure 3. Comparison of the estimated and true response for the unmeasured DOFs with 10% added noise using initial guess 200% of exact parameter values: (a) 2nd DOF; (b) 3rd DOF.

4 CONCLUSIONS

This research develops and identification method for the estimation of stiffness and Rayleigh damping coefficients of a four degree of freedom shear linear model that represents the CWH base isolated building. Numerical proof of concept and validation showed that the estimated structural stiffness and damping coefficients converge to the exact values using different initial guesses without measurement noise. The identification results with 10% added noise show that initial guesses of the estimated parameters affect the identification accuracy with measurement noise. Finally, the estimated response matched well with the simulated true response for the unrecorded degree of freedoms, even with added noise using an initial guess of 200% of the exact value. Thus, the identification procedure is capable of identifying the stiffness and damping coefficients and predicting the unrecorded structural response accurately for the proposed shear linear model with a limited number of sensors.

5 ACKNOWLEDGEMENTS

The China Scholarship Council (No. 201306260119) in support of this study is greatly acknowledged.

6 REFERENCES

Boroschek, R.L., Moroni, M.O. & Sarrazin, M. 2003. Dynamic characteristics of a long span seismic isolated bridge, *Engineering Structures*, 25(12): 1479-1490.

Chaudhary, M.T.A., Abe, M., Fujino, Y. & Yoshida, J. 2000. System identification of two base-isolated bridges using seismic records, *Journal of Structural Engineering*, 126(10): 1187-1195.

Chen, J., Liu, W., Peng, Y. & Li, J. 2007. Stochastic seismic response and reliability analysis of base-isolated structures, *Journal of Earthquake Engineering*, 11(6): 903-924.

Furukawa, T., Ito, M., Izawa, K. & Noori, M.N. 2005. System identification of base-isolated building using seismic response data, *Journal of engineering mechanics*, 131(3): 268-275.

Gavin, H.P. & Wilkinson, G. 2010. Preliminary Observations of the Effects of the 2010 Darfield Earthquake on the Base-Isolated Christchurch Women's Hospital, *Bulletin of the New Zealand Society for Earthquake Engineering*, 43(4): 360-367.

Hijikata, K., Takahashi, M., Aoyagi, T. & Mashimo, M. 2011. Behavior of a base isolated building at Fukushima Dai-Ichi Nuclear Power Plant during the Great East Japan Earthquake, *Proc. of the International Symposium on Engineering Lessons Learned from the 2011 Great East Japan Earthquake*, Tokyo, Japan, pp. 1542-1551.

Huang, M.-C., Wang, Y.-P., Chang, J.-R. & Chen, Y.-H. 2009. Physical-Parameter Identification of Base-Isolated Buildings Using Backbone Curves, *Journal of structural engineering*, 135(9): 1107-1114.

Kuang, A., Sridhar, A., Garven, J., Gutschmidt, S., Rodgers, G.W., Chase, J.G., Gavin, H.P., Nigbor, R. & Macrae, G. 2014. Christchurch Women's Hosptial: performance analysis of the base-isolation system during the series of Canterbury Earthquakes 2011-2012, University of Canterbury, Christchurch, New Zealand

Kulkarni, J.A. & Jangid, R. 2003. Effects of superstructure flexibility on the response of base-isolated structures, *Shock and Vibration*, 10(1): 1-13.

Kulkarni, J.A. & Jangid, R. 2002. Rigid body response of base‐isolated structures, *Journal of structural control*, 9(3): 171-188.

Matsagar, V.A. & Jangid, R. 2008. Base isolation for seismic retrofitting of structures, *Practice Periodical on Structural Design and Construction*, 13(4): 175-185.

Miwada, G., Yoshida, O., Ishikawa, R. & Nakamura, M. 2012. Observation records of base-isolated buildings in strong motion area during the 2011 Off the Pacific Coast of Tohuku earthquake, *Proc. of the International Symposium on Engineering Lessons Learned from the 2011 Great East Japan Earthquake*, Tokyo, Japan, pp. 1017-1024.

Nagarajaiah, S. & Sun, X. 2000. Response of base-isolated USC hospital building in Northridge earthquake, *Journal of structural engineering*, 126(10): 1177-1186.

Park, Y., Wen, Y. & Ang, A. 1986. Random vibration of hysteretic systems under bi‐directional ground motions, *Earthquake engineering & structural dynamics*, 14(4): 543-557.

Sridhar, A., Kuang, A., Garven, J., Gutschmidt, S., Chase, J.G., Gavin, H.P., Nigbor, R.L., Rodgers, G.W. & MacRae, G.A. 2014. Christchurch Women's Hospital: Analysis of Measured Earthquake Data during the 2011-2012 Christchurch Earthquakes, *Earthquake Spectra*, 30(1): 383-400.

Stewart, J.P., Conte, J.P. & Aiken, I.D. 1999. Observed behavior of seismically isolated buildings, *Journal of Structural Engineering*, 125(9): 955-964.

Xu, C., Chase, J.G. & Rodgers, G.W. 2014. Physical parameter identification of nonlinear base-isolated buildings using seismic response data, *Computers & Structures*, 145(1): 47-57.

Yang, J.N., Lei, Y., Pan, S. & Huang, N. 2003. System identification of linear structures based on Hilbert–Huang spectral analysis. Part 1: normal modes, *Earthquake engineering & structural dynamics*, 32(9): 1443-1467.